Review

Recent advances in post-synthetic modification of metal–organic frameworks: New types and tandem reactions

Zheng Yin [c], Shuang Wan [b], Jian Yang [b], Mohamedally Kurmoo [d], Ming-Hua Zeng [a,b,*]

[a] Key Laboratory for the Chemistry and Molecular Engineering of Medicinal Resources, School of Chemistry and Pharmaceutical Sciences, Guangxi Normal University, Guilin 541004, PR China
[b] Hubei Collaborative Innovation Center for Advanced Organic Chemical Materials, Ministry-of-Education Key Laboratory for the Synthesis and Application of Organic Functional Molecules, College of Chemistry and Chemical Engineering, Hubei University, Wuhan 430062, China
[c] College of Chemistry and Chemical Engineering, Shaanxi University of Science and Technology, Xi'an 710021, PR China
[d] Institut de Chimie de Strasbourg, CNRS-UMR 7177, Université de Strasbourg, 67070 Strasbourg, France

ARTICLE INFO

ABSTRACT

In the past five years, post-synthetic modification (PSM) has become a very useful strategy in systematically functionalizing metal–organic frameworks (MOFs) by modifying the linker, metal node, pore character, and surface environment for the purpose of increasing the structural stability and introducing desired properties. In this review, we intend to demonstrate the two major trends in PSM including the mushrooming of new types of reaction and the combination of multi-steps PSM. The selected examples illustrate three promising PSM classes, post-synthetic metal exchange (PSME), post-synthetic ligand exchange (PSLE) and post-synthetic elimination and insertion (PSE&I). Combined with the well-developed covalent PSM and dative PSM, tandem PSM which constitutes of multistep and different types of reaction adds to the step-by-step improvement of catalytic activity, regulating magnetism and others. These recent advances in PSM not only open new paths to improve the function of MOFs, but also reveal the unprecedented reaction complexity of crystalline solids.

© 2017 Elsevier B.V. All rights reserved.

Contents

1. Introduction

Metal–organic frameworks (MOFs) are hybrid compounds where metal nodes are linked into infinite arrays through multi-topic ligands. These crystalline solids with accessible open spaces have rapidly grown into a major area of chemical research attracting interest and enthusiasm from a wide community over the past two decades [1–2]. Advances have been made in synthesis, crystal engineering, functionality and applicability of MOFs [3–18]. Even so, achieving desired MOF structures with targeted properties and functions still present a significant challenge, which sets the foundation for major improvement for future industrial application of these promising materials.

Coupled with the advances in synthesis and functionalization of MOF, post-synthetic modification (PSM) has drawn great attention as an efficient and flexible tool to alter the structure and properties of MOF (Fig. 1) [19–26]. The concept of PSM, that is performing reaction in a post-synthetic manner, appeared at the development stage of MOF [27]. Following some early examples, Cohen used PSM to describe the reaction between IRMOF-3 and acetic anhydride which produce the modified framework containing newly formed amide group in 2007 [28–30]. Soon, such a unique strategy exhibits its great potential in systematically modifying the structure of MOF and facilitating the generation of functional MOF not accessible from direct synthesis. Several researchers around the world were attracted to this area in the following years. As a rough estimation, there are more than 300 hits for PSM in *Scifinder* database and is steadily growing.

These reports presented crucial and common features of PSM differing from other chemical reactions [19]. The reactant goes through the pores into the interior of the MOF to react with either the ligand or the metal nodes. The connection and topology of the parent MOF is not altered after the reaction. Solid-solution reactions were widely applied where the MOF crystals were soaked in a solution containing the reactants. Though solid–gas and solid–solid reaction are less common they are also possible processes for PSM [31–33]. Different from decomposition-reconstruction, the crystalline state is retained without changes in morphology of the crystals. The single-crystal-to-single-crystal (SC–SC) transformation is quite helpful for the structure resolution [34]. There are great changes in the linker functional group and metal coordination/geometry/valence. As a result, modification of the pores, surface, stability, hydrophobicity, sorption, catalysis properties, luminescence, and magnetism can be realized by changes of the structure.

MOF can be modified in many different ways. Based on the breaking and forming of chemical bonds, PSM were divided into covalent PSM, dative PSM and post-synthetic deprotection (PSD). These reactions occupy the vast majority of PSM and have been summarized in 2012 by Cohen [20]. Since then, various new PSM types have sprung up. These reactions cover metal ions exchange within the framework known as transmetalation, post-synthetic metalation or post-synthetic metal exchange (PSME) [21–24]. The substitute of the ligand of a MOF by solid-solution reaction is defined as solvent-assisted linker exchange (SALE), or post-synthetic ligand exchange (PSLE) [25]. When symmetry, size, coordination are compatible, low-connected MOF transform to another MOF with high-connection numbers, through a process of sequential linker installation (SLI), or post-synthetic installation (PSI) [26]. Post-synthetic polymerization (PSP) of a MOF with monomer

2008
SM Cohen: The first example of tandem PSM on MOF that two sequential steps acetylation of IR-MOF-3.

2012
SM Cohen: Comprehensive summary of covalent PSM and dative PSM.

JT Hupp: Imidazolate linker exchange in ZIFs.

2014
QW Li: Creation of ordered vacancies by post-synthetic elimination.

MH Zeng: Modulation of four magnetic ground states on MOF by tandem PSM.

2016
OM Yaghi: Seven post-synthetic covalent reactions in tandem on IRMOF-74-III.

2007   2012   2017

2007
SM Cohen: The first example of PSM that acetylation of IRMOF-3.

HW Hou: Cu²⁺, Pb²⁺ substitute the single node of Cd²⁺ in a pillared bilayer MOF.

JR Long: Cu²⁺, Zn²⁺ partly substitute the [Mn₄Cl] SBU of negative 3D framework of Mn-BTT.

2011
W Choe: The first example of post-synthetic linker exchange on MOF. Pillar dipyridine replacement in extended 2D and 3D MOFs.

2013
NL Rosi: Dicarboxylate exchange on octa-nuclear SBU based MOFs to systematically increase the pore dimensions.

MH Zeng: Interior and surface modification of MOF by tandem PSM.

2015
HC Zhou: Sequential linker installation in PCN-700.

JP Zhang: Post-synthetic ligand installation and cyclotrimerization in MIL-88B.

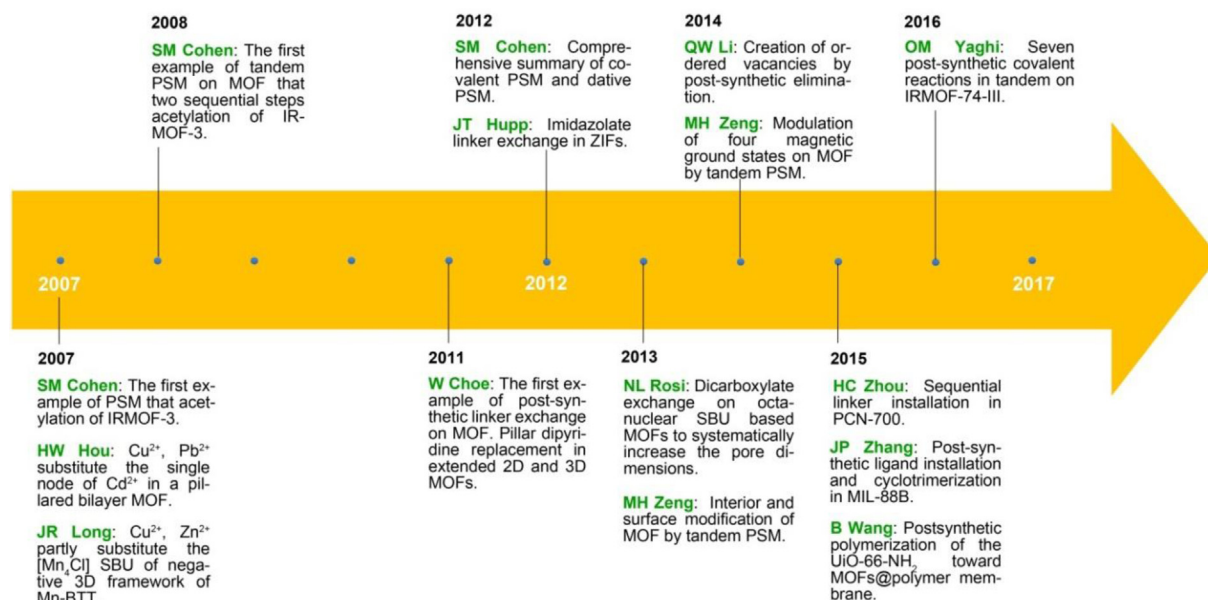**B Wang:** Postsynthetic polymerization of the UiO-66-NH₂ toward MOFs@polymer membrane.

Fig. 1. The history of development in PSM on MOFs with some representative works in the past decade.

initiator, and post-synthetic oxidation (PSO) of metal ions have also been reported very recently [26]. These new types of reaction performed on the selected MOF in post-synthetic fashion greatly broaden the concept of PSM.

Most reported PSM of MOF just involve one-step and one type of reaction with limited modification effect. Subsequently, the combined use of different PSM tools in a tandem way provides a chance to achieve targeted structures and functions that single-step PSM cannot realize. Numerous structural factors including part or whole of the framework, interior or surface of the crystals, aperture, shape, size of the pores, framework rigidity and flexibility, can be precisely modified in tandem manner. There are just limited reports in the literature realizing tandem PSM. Even so, the great significance and potential of tandem PSM were evidenced by the successful solving of those quite difficult problems including precise modulation of breathing behavior, step-by-step change of different magnetic ground states, introducing ordered vacancies and catalytic sites, producing multivariate MOF, and others.

The tendencies of exploring new types and tandem reactions become increasingly apparent in the past five years (Fig. 1). There are some reviews dealing with PSM focusing on different classifications. However, the above exciting tendency has not been clearly presented. We intend to highlight the representative breakthrough and latest advances on new types and tandem PSM based on selected works including several from China. The principles, research methods, modification effects on structure and function embedded in the PSM and our perspective will be summarized. The increased complexity in composition, structure and function generated by new types and tandem PSM is particularly important in advancing the chemistry of MOF.

2. New type post-synthetic modification (PSM)

Modifying the tagged group of the ligand hanging in the channels by reaction has dominated the early days of PSM, given the convenience to draw lessons from synthetic organic chemistry. Recently, the kinetically labile nature of metal–ligand coordination bonds in MOF has enabled exchanging both the metal ions and the organic linkers of MOF. Within some highly stable MOF, both the elimination and addition of multitopic linkers or metal ions are possible without destruction of the framework. Introducing suitable monomer to polymerize with the functional group of MOF presents a convenient method to prepare MOF@polymer hydrids.
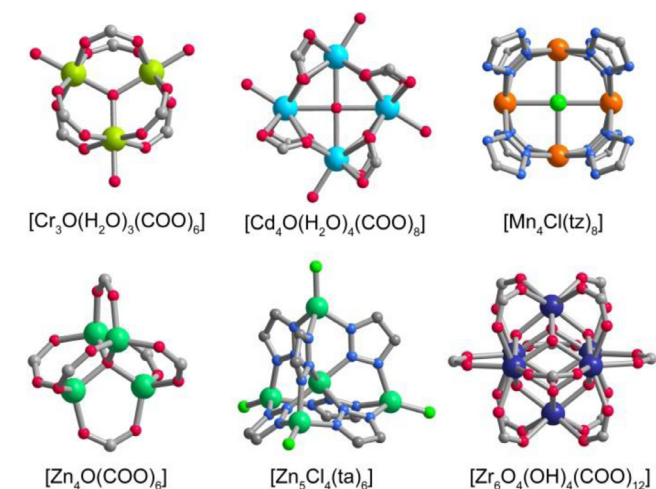

Fig. 2. The structures of typical polynuclear SBU in which the metal ions can be post-synthetically exchanged. General color code: C, gray; O, red; N, blue; Cr, lime; Cd, sky blue; Mn, orange; Zn, grass green; Zr, indigo.

The continuing emergence of new types of PSM enhances the range of reactivity of the crystalline solids.

2.1. Post-synthetic metal exchange (PSME)

Mutual replacement of metal ions is a common phenomenon in mineral. Cation doping is also widely employed for nanocrystals to tune their properties. Though cation exchanges in MOF were occasionally noticed at some single metal node MOF since 2007 [35], its general applicability in MOF with polynuclear secondary building unit (SBU) were only demonstrated very recently (Fig. 2).

A variety of dinuclear metal clusters, especially the $[M_2(COO)_4]$ paddle-wheel SBU, were found to be suitable for PSME. The successful examples have covered different MOF systems like (3,4)-connected *tbo* framework of Zn-HKUST-1, (3,24)-connected *rht* framework of Zn-PMOF-2 [36], PtS-type net of SNU-51 [37], (3,6)-connected *ith-d* framework of $[M_6(btb)_4(bpy)_3]$ (denoted as SUMOF-1 or FJI-1, bpy = 4,4′-dipyridyl) [38,39], (4,8)-connected *scu* framework of PCN-921 [40], and interpenetrating $[Zn_7(ptc)_3 (H_2O)_7][Zn_5(ptc)_3(H_2O)_5]$ ($H_4ptc = N$-phenyl-N'-phenyl bicyclo[2,2, 2]oct-7-ene-2,3,5,6-tetracarboxdiimide tetracarboxylic acid) constituted of both cationic and anionic frameworks [41]. In these MOF, a common feature is the replacement of Zn^{2+} by Cu^{2+} due to the comparable higher thermodynamic stability of the Cu SBU. The rigidity of the resulting framework is greatly increased. For example, the activation of Zn-HKUST-1 and Zn-PMOF-2 via the conventional vacuum drying is unsuccessful, leading to crystallinity loss and absence of significant N_2 sorption [36]. The inclusion of Cu^{2+} gradually restores the sorption capacity in a roughly linear tendency to the amount of Cu^{2+}. Multiple and reversible 3d transition metal ions exchange is successful in the SUMOF-1 [38,39], where the Zn^{2+} can be reversibly exchanged by Co^{2+}, Ni^{2+} and Cu^{2+}. Time dependent percentage conversion suggests relative stabilities of the clusters in an order of Co ≈ Ni < Zn < Cu. The PXRD, TGA and N_2 sorption results indicate framework stability follows the sequence of Zn ≈ Co ≪ Ni < Cu. Core–shell hybrid of SUMOF-1 with stable core and labile shell can be generated by epitaxial growth on seed crystals. By controlling the reaction parameters, complete metal exchange of the whole crystal or selective metal exchange of the external crystal lead to both homogeneous and heterogeneous compounds.

The metal exchange of trinuclear SBU was realized in both kinetically labile PCN-426-Mg and inert MIL-101(Cr) (Fig. 2) [42,43]. The latter is a rigid mesoporous solid, which is made of trimers of chromium octahedron. The Al^{3+} and Fe^{3+} replacement of MIL-101(Cr) was unambiguously proved by the peak shift on the UV–Vis reflectance spectra. After the cation exchange, the crystallinity of the parent crystal is maintained and with retention of the high porosity. By virtue of PSME, the Al^{3+} polymorph of MIL-101 unavailable by direct synthesis can be obtained. The feasibility of metal exchange in such a robust MOF inspires PSME as a universal tool for wide range of MOF.

Tetranuclear SBU is widely observed in various MOF. MOF-5 with $[Zn_4O(COO)_6]$ [44,45], $Cd_{1.5}(H_3O)_3[(Cd_4O)_3(hett)_8]$ [46], and $Mn_3[(Mn_4Cl)_3(btt)_8(CH_3OH)_{10}]_2$ (Mn-BTT) with $[Mn_4Cl]$ unit [47,48], were representative MOF template suitable for PSME (Fig. 2). Dincă's group investigated the substitution of di- and tri-valent metals into MOF-5 to give analogues, some of which are not accessible by typical synthetic pathways. Soaking MOF-5 into DMF saturated with different metal salts furnished metal exchanged M-MOF-5 ($M = V^{2+}$, Cr^{2+}, Mn^{2+}, Fe^{2+}, or Ni^{2+}) and ClMMOF-5 ($M = Ti^{3+}$, V^{3+}, or Cr^{3+}) [44,45]. The degree of substitution depends on the nature of each cation, concentration and reaction time. Under identical conditions, the substitution of Zn^{2+} ranges from less than 0.2 for Ti^{3+}, V^{2+} and V^{3+}, to 1.41 for Cr^{3+} per $[Zn_4O(COO)_6]$ SBU after one week. The reaction is homogeneous substitution occurring throughout the entire crystal

in SC–SC fashion. The resulting materials conserve both the morphology and the high porosity of MOF-5, though exchanges caused partial disruption and defects to the MOF lattice. Structure analysis shows the zinc metal node play a role of tridentate ligand for the pseudo-tetrahedral M^{2+}, and pseudo-trigonal bipyramidal M^{3+} with terminal chloride moieties. These inserted metal ions endowed MOF-5 with redox-active properties. The substituted Cr^{2+} in MOF-5 can be oxidized by $NOBF_4$, while NO can be activated by the Fe^{2+}-substituted MOF-5 and generate a rare Fe^{III}-nitrosyl compound.

The Mn-BTT is an anionic SOD-type MOF constructed from $[Mn_4Cl(tz)_8]^-$ unit with high density of exposed metal cation on the pore surface. The replacement of guest Mn^{2+} ions by several metal ions leads to variation of the H_2 sorption enthalpy [47]. Except for the guest Mn^{2+}, Cu^{2+} and Zn^{2+} can partly replace the Mn^{2+} within the tetranuclear cluster of Mn-BTT. The direct synthesis under similar conditions did not generate the Zn-based analogue. By optimizing reaction conditions to improve percentage conversion, the post-synthetic Zn^{2+} exchange would be helpful to obtain the Zn-MTT. DFT calculation shows the $[Zn_4Cl(tz)_8]^-$ would exhibit a considerably higher binding energy compared to that of Cu^{2+}, Mn^{2+} and Fe^{2+} based compounds [48].

The metal exchange in penta- and hexa-nuclear MOF were found in MFU-4l and UiO-66(Zr) (Fig. 2). MFU-4l constructed from pentanuclear T_d symmetrical $[Zn^{oct}Zn_4^{tet}Cl_4(ta)_6]$ (oct, octahedral; tet, tetrahedral; ta, triazolate ligand) SBU, is an interesting MOF possessing large porosity and unsaturated metal sites [49]. The Zn^{2+} of MFU-4l can be replaced by Co^{2+} in DMF and the conversion is greatly affected by the metal ratio of the starting mixture. The excess of Co^{2+} leads to replacement of all the outer tetrahedral Zn^{2+} with retention of the central octahedral Zn^{2+}. The resulting Co-Zn-MFU-4l was expected to be a prototypic MOF comprising redox reversibility, thermal stability, and robustness required for a catalytic MOF.

UiO-66(Zr) with $[Zr_6O_4(OH)_4(COO)_{12}]$ SBU is well known for its high structural stability under a variety of chemical conditions [50]. As lighter and highly oxophilic metal of Ti^{4+}, the Ti(IV)-MOF was attractive because of the improved stability and its unique photochemical activity. Soaking particles of UiO-66(Zr) into DMF containing Ti(IV) or Hf(IV) ions under mild heating, leads to substitution of the Zr^{4+} [51]. Positive-ion aerosol time-of-flight mass spectrometry (ATOFMS) spectra reveals the incorporation was achieved with $TiCl_4(THF)_4$, giving >90% Ti^{4+} conversion of the starting particles (~38 wt% for whole sample). Similar experiment but higher reaction temperature with $HfCl_4$ leads to lower Hf^{4+} conversion of ~20% for the MOF particles.

Except for the above polynuclear MOF, recent advances show PSME is feasible in MOF-74-Mg and MIL-53-Al/Fe with 1D chain SBU [51,52]. The post-synthetic reaction of MOF-74-Mg with Ni^{2+} in weakly acid condition generated MOF-74-Ni/Mg with 70 mol% Ni^{2+} content. The reaction is dominated by both predominant cation exchange and partly crystallization. Though the Ni^{2+} distributed over the whole crystal, the Ni/Mg ratio decreased from exterior to interior. The Ni-substituted MOF-74 exhibits better adsorption ability than unmodified compound, as the PSME makes the surface more stable upon similar thermal activation process.

PSME was also used in porphyrin-encapsulated MOF to alter the properties. $[Cd_6(bpt)_4Cl_4(H_2O)_4]$ (porph@MOM-10, H_3bpt = biphenyl-3,4',5-tricarboxylate) is a porous and ionic framework with $[Cd_3Cl_2(COO)_6]$ SBU [53]. Counterions of CdTMPyP cluster (TMPyP = meso-tetra(N-methyl-4-pyridyl)porphyrin tetratosylate) were encapsulated in the framework. Both the Cd^{2+} in the framework and CdTMPyP cation can be exchanged by Mn^{2+} and Cu^{2+}, giving Mn^{2+} completely exchanged and Cu^{2+} partly exchanged products. To catalyze the epoxidation of trans-stilbene, the Mn- and Cu-based MOF exhibit much higher conversion compared to the parent MOF. Similar Cd^{2+} to Cu^{2+} exchange is observed in
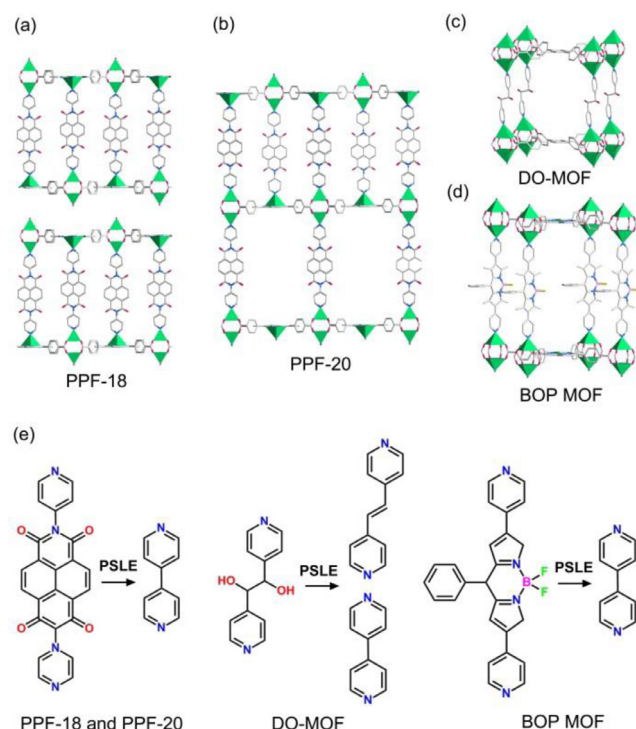

Fig. 3. Views of the pillared-layer motifs of PPF-18 (a), PPF-20 (b), DO-MOF (c), BOP MOF (d) and the post-synthetic ligand exchange in the MOF (e).

porph@MOM-11 [54]. Interestingly, PSME also induces a SBU transformation from dinuclear $[Cd_2(COO)_6]$ to tetranuclear $[Cu_4X_2(COO)_6]$. The relatively larger Cu-SBU permits a unit cell expansion up to 20%, affording higher surface area and larger pore size.

2.2. Post-synthetic ligand exchange (PSLE)

PSLE represents the exchange of the key extending ligand of a framework by another similar ligand of different length or functional group, with the retention of the MOF topology. The exchange of anionic carboxylate has been found in a few 0D cluster and 2D layer [55,56]. However, the major breakthrough of PSLE in infinite 3D MOF was realized in 2011.

PPF-20 is a 3D extended framework where the paddle-wheel porphyrin layers are pillared by dpni (N,N'-di-4-pyridyl naphthalenetetracarboxydiimide) (Fig. 3b) [57]. Soaking PPF-20 into a replacement linker solution of bpy, the dpni pillar was replaced by bpy and isostructural PPF-4 was generated in SC–SC fashion. The exchange is quite quick and complete with 97% transformation accomplished after 2 h. As a result, the interlayer distance decreases from 21.2 to 12.8 Å. During the linker-replacement transformation, the parent MOF exhibits template effect to the daughter structure. The absence of side-shifting of the layers allows retention of the parent stacking sequence. Similar ligand exchange also succeeds in 2D bilayer of PPF-18, generating PPF-27 which is not attainable by direct synthesis (Fig. 3a).

Similar dipyridin exchange was achieved in other system. Hupp's group has synthesized a series of catenated or non-catenated frameworks from tetracarboxylic acid and dipyridyl ligands. The $[Zn_2(tcpb)(dped)]$ (DO-MOF, tcpb = 4,4',4'',4'''-benzene-1,2,4,5-tetrayl-tetrabenzoate, dped = 1,2-di(pyridin-4-yl)ethane-1,2-diol) is a pillared-layer MOF containing single framework and large void volume of 76%, due to H-bond interactions of the dped pillar (Fig. 3c). Both equal length 4,4'-azobis(pyridine) (abp) and shorter bpy can replace the dped struts of the parent
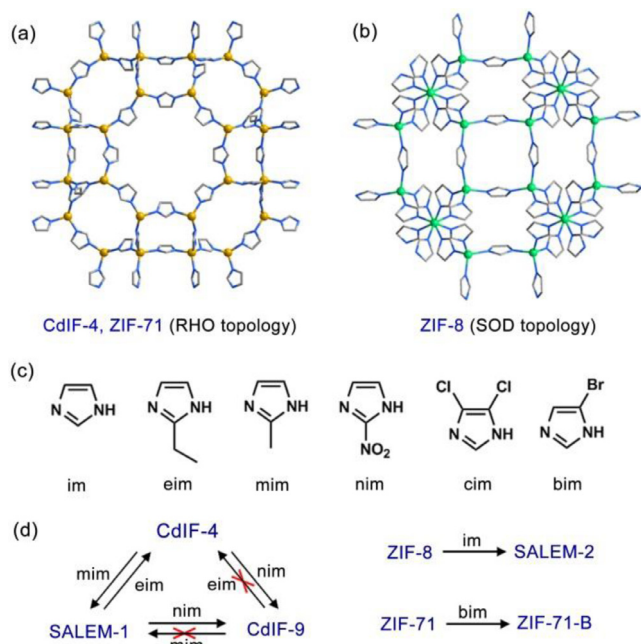
Fig. 4. (a) Perspective views of the CdIF-4 and ZIF-71 structures with RHO topology. (b) Perspective view of ZIF-8 structure with SOD topology. (c) View of imidazolate ligand with different substituted groups. (d) Post-synthetic ligand exchange in CdIF-4, ZIF-8 and ZIF-71.

Fig. 5. Post-synthetic dicarboxylate exchange in MIL-53(Al) (a) and MIL-68(In) (b) through a particle to particle fashion. Reproduced from Ref. [51] with permission of American Chemical Society.

DO-MOF, with 92% and 100% conversion, respectively [58]. The daughter MOF of SALEM-3 and SALEM-4 are non-catenated materials. However, isostructural pillared-paddle-wheel MOF with bpy and abp pillar is twofold interpenetrated compound in direct synthesis. The dipyridyl boron dipyrromethane (dbdp) pillar was also found replaceable by pyridine (py) in the light-harvesting BOB-MOF (Fig. 3d) [59].

Additional reports of ligand exchange were found in different systems including the robust MOF families. Zeolitic imidazolate frameworks (ZIF) are robust category of MOF because of the exceptionally strong metal-imidazolate bonds. Even so, PSLE has been realized in CdIF-4, ZIF-71 and ZIF-8 [51,60,61]. CdIF-4 with RHO framework is an attractive compound possessing several useful aspects like synthesis scalability, excellent purity and crystallinity. However, the large ethyl group of its 2-ethylimidazolate (eim) ligand limit the pore volume and hence the applications of CdIF-4. PSLE was found useful to the rich MOF family. Both 2-nitroimidazolate (nim) and 2-methylimidazolate (mim) can replace the pre-existing eim once CdIF-4 was soaked in heated DMF solution containing targeted ligands, generating CdIF-9 and SALEM-1 [60]. Reverse and serial PSLE can be accomplished with CdIF-4. The exchange between CdIF-4 and SALEM-1 is fully reversible, and it is also possible to transform SALEM-1 to CdIF-9 by soaking SALEM-1 in DMF solution containing eim and nim. However, reaction from CdIF-9 to CdIF-4 or SALEM-1 is not feasible under similar conditions. This was ascribed to the difference in Cd-imidazolate coordination strength and framework stability induced by substituent groups. For dichloro-substituted RHO-type ZIF-71, similar ligand exchange by 4-Br-1H-imidazole (bim) with nearly 30% conversion produces a new material that cannot be obtained by direct synthesis [51].

In more robust ZIF-8, [Zn(mim)$_2$], the replacement of the mim linkers with unsubstituted im and eim was reported [61]. ZIF-8 is an extensively studied iconic material featuring SOD topology and high void volume, which can be easily assembled into nanoparticle, thin-film, and membrane (Fig. 4b). However, the
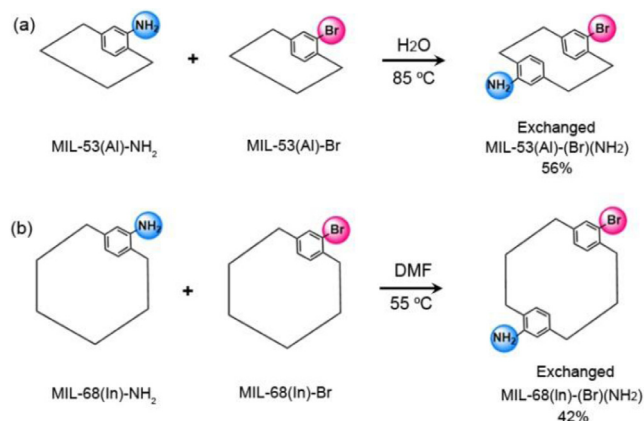
aperture diameter of 3.4 Å is too small due to the steric-hindrance of the methyl substituent. ZIF-8 with unsubstituted ligand is more attractive considering the unobstructed apertures and larger voids. However, various direct synthetic strategies for ZIF-8(im) have long been unsuccessful. Given that similar pKa values of Hmim and Him, the Zn-mim and Zn-im bonds in ZIF-8 may be exchanged. Even so, the ligand exchange required rather forcing conditions in solvent, concentration, temperature and time comparing to CdIF-4 and ZIF-71. The reaction parameters of solvent, ligand/MOF molar ratio, temperature and time were optimized to n-butanol, 6.7:1, 100 °C and 7 days, respectively. The resulting exchange of mim for im is up to 85% and generates the unreported isostructure of SALEM-2. Such ligand exchange is almost reversible with about 80% recovery of mim at similar reaction conditions. As expected, the new compound SALEM-2 not only retains the several advantages of ZIF-8 but also increases the pore window size and opens an additional aperture.

Apart from the above examples of exchange of dipyridyl and imidazolate linker, replacement of the linear dicarboxylate, one of the dominating ligands in MOFs, has emerged recently. Comparing to dipyridyl struts it is inherently more difficult for carboxylate exchange, because of the greater strength and complex bonding between a metal and the carboxylate ligand. The successful carboxylate exchange was surprisingly realized on some quite structurally stable MOF including [Al(OH)(bdc)] (MIL-53-Al, H$_2$bdc = benzene-1,4-dicarboxylic acid), [In(OH)(bdc)] (MIL-68-In), [Zr$_6$O$_4$(OH)$_4$(bdc)$_6$] (UiO-66-Zr), as well as complex polynuclear based MOF of Bio-MOF-101 (see later). Cohen et al. realized the ligand exchange of MIL-53-Al, MIL-68-In and UiO-66-Zr in both solid–liquid and solid–solid manner (Fig. 5) [51]. Br-bdc and NH$_2$-bdc based parent MOF microcrystals were independently suspended in solutions containing NH$_2$-bdc and Br-bdc, respectively. Though the framework connection and crystalline state is well retained, changes in composition of the MOF during reaction is revealed by ATOFMS results. Approximately more than half of the modified particles simultaneously give signals of bromine and nitrogen, suggesting the occurrence of ligand exchange. More interestingly, such ligand exchange can proceed in a solid-to-solid way. After suspending the mixture of Br-bdc and NH$_2$-bdc based UiO-66-Zr in water for 120 h, the ratio of particles underwent ligand exchange exceeds 50%. In addition, the role of solvent is quite important and no ligand exchange is observed in the absence of solvent. As a comparison, similar ligand exchange in [Cr$_3$F(H$_2$O)$_2$O(bdc)$_3$] (MIL-101-Cr) is not successful, as the inert Cr^{3+} node prevents the ligand exchange.
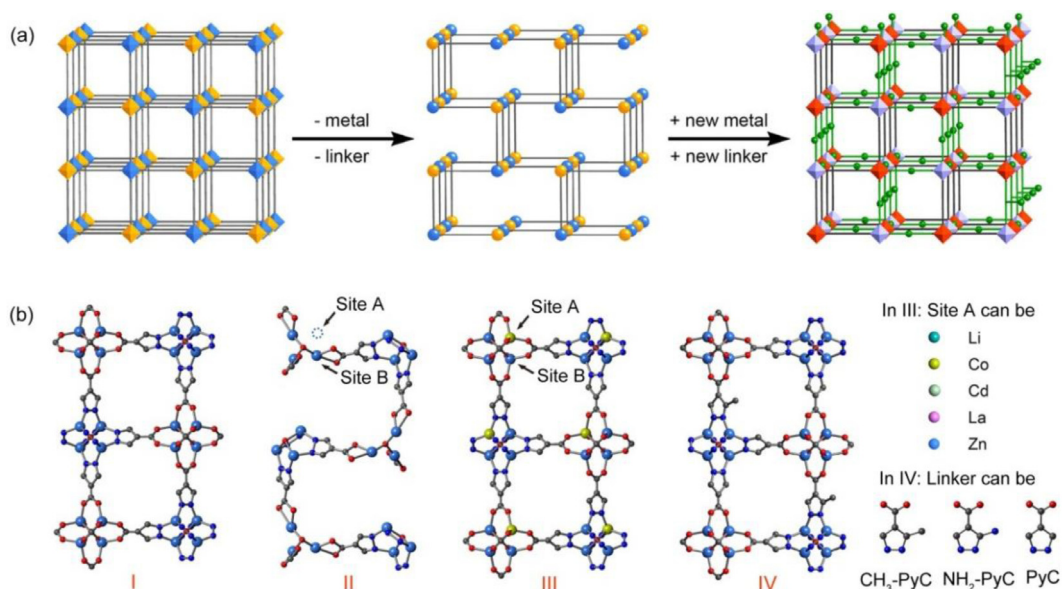
Fig. 6. (a) Schematic illustration of a framework undergoing metal and linker elimination/installation reactions. (b) Single-crystal structures of the MOF without vacancies (I), with vacancies (II), and with new modules filled in the vacancies (III and IV). Reproduced from Ref. [62] with permission of American Chemical Society.

Though reports are still limited, the successful ligand exchange in the above MOF systems suggests ligand exchange indeed would be a widespread phenomenon. Previous concept of rigidity and flexibility of MOF mainly stem from coordination distortion of the metal ions, curving/rotation/isomerization of the ligands, deformation/expansion/shrinking of the framework. The complex bonds broken and forming, both metal and/or ligand exchange during PSM provide a completely new perspective to consider the flexibility of MOF as crystalline solids. Deepening the research on post-synthetic exchanges not only benefits modification for targeted structure and function, but also help to understand the essence of coordination reaction and self-assemble of MOF.

2.3. Post-synthetic elimination and installation (PSE&I)

In some MOFs with multiply coordination bonds, there are great difference in bonding strength between the metal ions and ligands. As is widely observed, the terminal ligand of solvent can be removed by heating to generate open metal sites (OMS), without

Fig. 7. View of the post-synthetic insertion and in-situ cyclotrimerization in MIL-88-Fe. (a) The structure transformation from MIL-88 to ligand inserted 3-pyCN@MIL-88B and finally the MOF with the trimer. (b) The proposed process of the cyclotrimerization reaction. Reproduced from Ref. [64] with permission of Nature Publishing Group.

major distortion of the framework. Following this line, it is recently found that some linkers constituting the framework can be eliminated with coordination changes in the metal cluster but preservation of the infinite framework connection. For either of the above cases, if the coordination site of adjacent metal cluster matches well with an additional linker, post-synthetic installation may succeed to create a new MOF with higher connection numbers.

Li et al. reported the elimination and insertion of both ligand and metal ions in MOF-5 analogue of $[Zn_4O(PyC)_3]$ (PyC = 4-pyrazo lecarboxylate), where regular vacancies can be created (Fig. 6) [62]. The MOF processes two distinct but similar SBUs; that $[Zn_4O(COO)_6]$ formed exclusively from the carboxylate side of PyC and the $[Zn_4ON_{12}]$ from only the pyrazole end of PyC. When immersed in water, half of the linkers and a quarter of the Zn^{2+} were eliminated at a right time window. The resulting crystal of $[Zn_3\square_1(OH)(PyC)_{1.5}\square_{1.5}(OH)(H_2O)_{3.5}(PyC)_{0.5}]$ ($\square$, vacancy) process ordered metal vacancies and linker vacancies, with full retention of crystallinity. The structure transformation is achieved by taking out one Zn atom in each SBU and the excision of half of the linkers from the framework, with metal coordination saturation by H_2O. The new structure contains two kinds of triangular SBUs of $[Zn_3(OH)N_6]$ and $[Zn_3(OH)(COO)_3]$. Each SBU is connected to the remaining three organic linkers perpendicular to each other, resulting in a network with srs topology. The parent MOF features large and small pores (10.8 and 7.6 Å in diameter, respectively) with pore aperture of 4.5 Å in diameter. After creating vacancies, the resulting structure constitutes rectangular channels with the diagonal of the aperture ~13.0 Å. Acridine red of size $14.2 \times 8.3 \times 3.7$ Å^3 can diffuse into the pores of vacancies containing structure, but no diffusion into the original MOF. It was also found that the metal vacancies can be filled with other metal ions (Li^+, Co^{2+}, Cd^{2+}, and La^{3+}) and the linker vacancies with new functionalized linkers (CH_3-PyC and NH_2-PyC). The installation reactions can be carried out separately or in a combined step. The presented cycle of making a MOF without vacancies, creating ordered vacancies in that MOF, and filling such vacancies with new modules is fundamentally important given that it generates more complex MOF which otherwise cannot be made.

In another work, Zhang group reported the elimination and installation in the quite flexible $[Fe_3O(bdc)_3X(H_2O)_2]$ (MIL-88B,

Fig. 8. (a) Perspective structure of the PCN-700 with two different pockets of A and B between adjacent clusters. (b) Dicarboxylate ligands of different lengths which have been inserted into PCN-700.

X = OH⁻/F⁻/Cl⁻) (Fig. 7) [63,64]. MIL-88 is built from trimeric SBU and linear dicarboxylate ligands, possessing 1D nanosized hexagonal channels. It is found that the terminal ligands can be removed or exchanged leaving potential OMS. These OMS adopt C_3 symmetry and locate at the same height along the channels. Such special OMS geometry is used to fix three terminal ligands and then facilitate subsequent cyclotrimerization reactions. Di-functional ligand with pyridyl and unsaturated alkene/alkyne group of 4-cyanopyridine, 4-ethynylpyridine and 4-vinylpyridine were inserted into the channels through the pyridyl donor. Further heating the modified MOF at 140 °C, results in the cyclotrimerization reactions of the inserted ligands. Evidence from single-crystal diffraction, IR, ESI-MS, and NMR confirmed the high yield formation of cyclic trimers inside the channels. Further study shows it is the perfect coordination geometry on the OMS forces the three unsaturated groups to gather at desired positions for thermal induced cycloaddition reaction. The trimerization reaction has high requirement for the inserted ligands. Control reaction did not work for monomers without suitable coordination sites or geometry. Because of the coordination of the large trimers within the channels, the parent framework greatly expands to 145% in cell volume compared to the most shrunken forms of MIL-88B. In addition, the flexible parent MOF turn to a highly rigid framework with increased sorption capacity.

PCN-700 is another prototype MOF suitable for PSE&I reaction, which have been well studied. It is an 8-connected *bcu* MOF based on [Zr₆O₄(OH)₈(H₂O)₄] SBU (Fig. 8). Each Zr₆ cluster is connected to eight Me₂-bpdc (H₂Me₂-bpdc = 2,2′-disubstituted biphenyl-4,4′-di carboxylic acid) linkers above and below the equatorial plane. The space between two adjacent Zr₆ clusters in the equatorial plane is a natural "pocket" for the accommodation of one linear dicarboxylate linker by replacing the terminal OH⁻/H₂O. The two pockets (16.4 Å for A and 7.0 Å for B) make it possible to sequentially install two different linkers. The highly stable PCN-700 with certain flexibility allows the structure to self-adjust according to the linkers. Exposing PCN-700 crystals to solutions of H₂bdc (6.9 Å) and H₂Me₂-tpdc (15.2 Å, H₂Me₂-tpdc = 2′,5′-dimethylterphenyl-4,4″-dicarboxylate) in DMF at 75 °C, PCN-701 with inserted bdc, PCN-702 with inserted Me₂-tpdc, PCN-703 with both bdc and Me₂-tpdc was obtained depending on the reaction procedure [65]. The existence and position of inserted ligand are unambiguously observed in the crystallographically resolved structure. The

crystallinity and porosity is well maintained after ligand insertion. The sequence of the ligand installation is crucial for the success formation of PCN-703. Starting with a short linker, the bdc will occupy all the small pockets B, leaving the slightly changed pocket A unoccupied and large enough to install Me₂-tpdc. However, if the longer Me₂-tpdc is installed first, they will occupy all the pockets A and meanwhile stretch the pocket B, impossible to install bdc. Following this strategy, combinations of fa (fumarate), bdc, ndc, bpdc (4,4′-biphenyldicarboxylate), tpdc and bddc (4,4′-(1,3-butadiyne-1,4-diyl)bis(3-methylbenzoate)) can be installed into PCN-700 according a geometric analysis [66]. Installation of single linker into PCN-700 generates two-linker MOF, namely [Zr₆O₄(OH)₆(H₂-O)₂(Me₂-bpdc)₄L] (L = fa, bdc, ndc, bpdc), which is 10-connected *bct* net. When two different linkers were installed, 11-connected *ela* framework of [Zr₆O₄(OH)₅(H₂O)(Me₂-bpdc)₄LL′₀.₅] (L = bdc or ndc, L′ = tpdc) was obtained, where two of the three pockets are inserted. The third remaining pocket mismatches other ligands thus no linker is further installed. If all the three pockets are simultaneously occupied, the resulting compound is a 12-connected framework of [Zr₆O₄(OH)₄(Me₂-bpdc)₄LL′] (L = bdc, L′ = bddc; L = ndc, L′ = bddc; L = bpdc, L′ = tpdc).

Adapting similar strategy, Su et al. reported the modification on breathing behavior of LIFM-28, a PCN-700 analogue constructed from 2,2′-bis(trifluoromethyl)-4,4′-biphenyldicarboxylate (btbc)

Fig. 9. View of two-step tandem PSM to introduce functional group like: -dibromine (a), -triazole (b), -diamine (c), -α amine-β-hydroxy (d), and -sulfonic acid (e).

[67]. LIFM-28 is a highly flexible compound which is structurally sensitive to the departure or inclusion of solvent molecules. There are reversible transformation between the original phase and a denser phase. The dicarboxylate installation on the smaller pocket causes ligand-dependent deformation along the *c*-axis, while the larger pocket is unoccupied with remaining pores for functional modification. A series of isoreticular MOF of LIFM-29 to LIFM-33 were obtained. In contrast, elimination of the installed linker in acid/basic aqueous solution can recover the LIFM-28, except for LIFM-33 with –NH$_2$ group. The installed linkers bring different elastic deformation effect. It was found that two shorter spacers lead to pore contraction, while three longer linkers cause large expansion which surpasses the structural changing magnitude induced by solvent. The stepwise installation/uninstallation of ligand with different lengths is used to control the structural breathing behavior in a continuous fashion. As a result, the modified MOF exhibits much better performance in gas sorption and separation.

3. Tandem PSM

3.1. Introduction of functional groups by tandem PSM

Introducing functional groups into the skeleton of MOF is very important as the introduced groups affect application in sorption, separation, catalysis and others. Tandem PSM help to produce MOF possessing multiple functionalities which are otherwise difficult or infeasible to acquire by direct synthetic methods.

Cohen presented the primitive tandem PSM, where crotonic anhydride stoichiometric convert all the amino groups of IRMOF-3 to generate IRMOF-3-AMCrot in the first step (Fig. 9a) [68]. Then the IRMOF-3-AMCrot crystals were exposed to bromine in CHCl$_3$. By controlling reaction time, various modified MOFs with different bromination degree can be obtained. In another early example, the DMOF-NH$_2$ was treated with tBuONO and TMSN$_3$ to produce the corresponding azide intermediate of DMOF-N$_3$ (Fig. 9b) [69]. Then the triazole modified DMOF-fun is produced by cycloaddition reaction with phenylacetylene catalyzed by CuI(CH$_3$CN)$_4$PF$_6$. Rieger et al. has used tandem PSM to introduce molecular gates and selectivity tuning of CO$_2$ over N$_2$ sorption into the modified UiO-66 analogue (Fig. 9c, d) [70]. Through high conversion reaction including bromination, epoxidation with dimethyldioxirane, the UiO-66 with allylic side chains converted to MOF with dibromide and epoxide substituent. The subsequent reaction of the modified crystals with NH$_3$ introduce vicinal 1,2-diamino and vicinal amino alcohol functionality into the MOF, which cannot be obtained by direct synthesis. The resulting epoxide modified compound displayed gated pores and negligible adsorption of N$_2$. While, the CO$_2$ capture of the aminoalcohol modified MOF was about four times higher compared to the starting compound. Starting from MIL-101-NO$_2$, Gao et al. produced dually functionalized MOF with both amino and sulfo groups through tandem PSM (Fig. 9e). MIL-101-NO$_2$ was first reduced to MIL-101-NH$_2$, followed with the ring-opening reaction of 1,3-propanesulfone with the amino group [71]. By controlling the reaction time and the dosage of 1,3-propanesulfone, different ratios of sulfo-modified linker can be realized. The resulting zwitterionic MOF exhibits acid-base catalytic performance, with the ammonium group being the catalytic acid site and catalyze deacetalization, and the base sites catalyze Knoevenagel condensation.

Based on the frequent two-steps tandem PSM, multistep reactions were reported. A three step tandem PSM was realized in a high stable compound of [Cr$_3$F(H$_2$O)$_2$(μ$_3$-O)(O$_2$CC$_6$H$_4$CO$_2$)$_3$] (MIL-101-Cr) [72]. A NO$_2$ functionality was first introduced to linker of the parent MOF, by harsh reaction with concentrated nitric acid and sulfuric acid. In the second step, SnCl$_2$ reduced the nitro
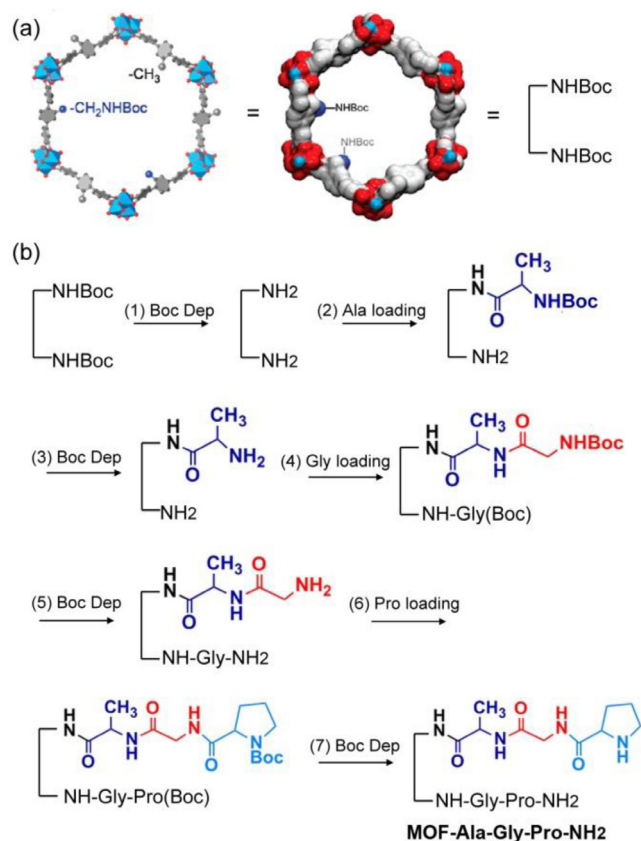

Fig. 10. View of seven-step tandem post-synthetic modification to introduce functional group in MOF-74(Mg)-III. Reproduced from Ref. [74] with permission of American Chemical Society.

to amino groups and yield Cr-MIL-101-NH$_2$, on which the third step of acylation can be conducted with ethyl isocyanate. Starting from IRMOF-3, a set of multifunctional MOFs with as many as five different substituents, that is NH$_2$ and amide with different branch chain, can be prepared by four-steps tandem PSM [73]. Yaghi group recently presents an example that contains as many as seven sequential reaction steps (Fig. 10) [74]. A mixed-ligand version of MOF-74(Mg)-III, containing 3,3″-dihydroxy-(1,1′:4′,1″-terphenyl)-4,4″-dicarboxate (dtdc) and 40% Boc-protected (Boc = *tert*-butyloxycarbonyl) amine derivative, was selected as the parent MOF. It is highly porous with massive 25 Å 1D channels that can accommodate sterically demanding reactions. The MOF was
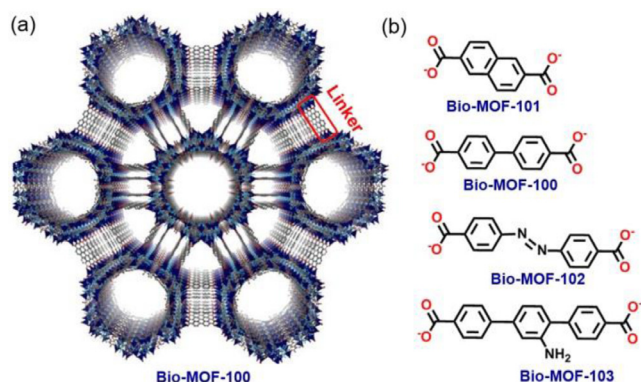

Fig. 11. (a) Structure projection of the mesoporous Bio-MOF-100. (b) The step-by-step post-synthetic ligand exchange starting from Bio-MOF-101.

subjected to a series of deprotection and peptide coupling reactions, generating tripeptides within the large pores. The multiple reaction cycles resulted in a heterogeneous mixture of peptides within the MOF. The final modified MOF-Ala-Gly-Pro-NH$_2$ with 20% loading onto the linker was shown to be a efficient catalyst for the α-chlorination of butyraldehyde. Presumably due to confinement effects within the MOF pores, the resulting MOF-based catalyst showed improved enantioselectivity compared with a homogeneous analogue (20% *vs* 2% *ee*). In addition, MOF-Asp-His-Cys-NH$_2$ with 10% loading onto the linker displays measurable protease activity on a model pentapeptide substrate.

3.2. Engineering porosity and pores by tandem PSM

One of the primary goals of PSM has been the modification of the porosity and pore surface of the parent MOF. It is mainly achieved by various covalent PSM to change the functional group of the linker. Both increased and decreased porosity can be obtained depending on the size and spatial configuration of the modified groups. However, the change in porosity is moderate and is limited by the constant topology of the framework. Since the appearance of PSLE, introducing linker of different length or functionality by tandem PSM into the selected framework helps to systematically engineering the porosity and pores.

One impressive work adapting the above strategy is the preparation of isoreticular analogues of a highly porous framework of [Zn$_8$(ad)$_4$(bpdc)$_6$O$_2$]·guest (ad = adeninate, BioMOF-100) (Fig. 11) [75–77]. It is an anionic and mesoporous MOF constructed from large [Zn$_8$Ad$_4$O$_2$]$^{8+}$ building units. Due to the exclusively mesoporous channels running along three different directions, the compound exhibits quite high surface area, large pore volume and low densities. It is expected that the porosity of Bio-MOF-100 would further greatly increase once the shorter ligand are replaced by longer one. However, it is also known the direct synthesis of these extremely porous framework with longer linker is not easy, especially in such a mixed linker MOF [78]. The direct synthesis of BioMOF-101 with shorter linker of 2,6-naphthalene-dicarboxylate (ndc) is successful. Unfortunately, it is not possible to directly obtain targeted isostructural MOF with longer ligand. Direct exchange of longer dicarboxylate work well in this system and extremely porous MOFs with increased mesoporous cavities were produced. The nearly complete ligand exchange results in structure evolution for the entire crystal, coupling with volume expansion of the solid phase. The new members of BioMOF-102 and BioMOF-103, shows increased mesoporosity high to 4.36 and 4.13 cm^3/g, which represent the most porous MOF even for organizing large molecules like enzyme. Following such tandem PSLE strategy, mono-, di- and trifunctionalization in BioMOF-100 were realized, in which the ratios of orthogonal functional groups (–N$_3$, –CHO, –NH$_2$) are tunable with reaction time [76]. Subsequently dye-quencher modification and spectrophotometric analysis suggests a random distribution of the functional groups in the binary BioMOF-100. Because the PSLE proceeds from surface to core of the crystal, new heterogeneously porous MOFs with internal pore gradients can be prepared, upon halting the ligand exchange reaction [77]. The nature of PSLE allow preparation MOF that may be thermodynamically or interpenetration unfavorable. It is believed tandem PSLE would be a potentially universal method to systematically adjust the pore dimensions of MOF.

3.3. Improving structural stability by tandem PSM

Low structure rigidity and difficulty in activation restrict the application of some highly porous MOF. The combination of hard Lewis bases of carboxylate group with hard Lewis acids like Cr^{3+}, Zr^{4+}, or Ti^{4+} benefits the formation of stable MOF, as confirmed in the UiO-66(Zr), MIL-53(Cr) families [79]. As mentioned above in PSME, replacing of Zn^{2+} by Cu^{2+} always increase the structural stability of MOF. However, the direct introduction of target metal ions may be subjected to low exchange rate, uncompleted conversion, decomposition of the MOF and others. Based on exchanging mechanism of different metal ions, tandem PSME is useful to improve structural stability.

PCN-426-Mg is a kinetically labile MOF constructed from [Mg$_3$(μ_3-O)] cluster and tetracarboxylate [42]. It is dissolved immediately after immersion in water, and collapsed after activation and failed to exhibit permanent porosity. High valence metal like Fe^{3+} and Cr^{3+} were expected to replace the Mg^{2+} and increase the rigidity of the framework. Direct metal exchange of PCN-426-Mg with anhydrous FeCl$_3$ revealed 87% introduction of Fe^{3+}, but the crystal become opaque. As a comparison, only a trace amount of Cr^{3+} were exchanged, given the kinetically inert d^3 configuration results in a much slower reaction rate constant. In addition to the incomplete metal exchange, the PXRD pattern also indicates framework decomposition after Mg^{2+}/Fe^{3+} exchange. It seems direct metal exchange of Fe^{3+} or Cr^{3+} is not a suitable route toward stable high valence MOF. One-pot solvothermal reactions of the ligand with FeCl$_3$ and CrCl$_3$, also failed to yield a crystalline product. On this occasion, PCN-426-Mg was completely exchanged with FeCl$_2$ in 3 h under the protection of nitrogen, coupling with colorless to purple color change of the crystals. Subsequently, the PCN-426-Fe(II) crystals was suspended in DMF and bubbled with an air stream for 15 min, generating the targeted PCN-426-Fe(III) by a post-synthetic oxidation reaction in SC–SC fashion. PCN-426-Cr(III) was synthesized through the same tandem method using anhydrous CrCl$_2$. The resulting framework exhibits greatly improved stability. The crystallinity of PCN-426-Cr(III) keeps intact within pH = 12 to extremely acidic conditions of 4 M HCl for at least 12 h. Both PCN-426-Fe(III) and PCN-426-Cr(III) shows high porosity with BET surface areas of 2132 and 3155 m^2 g^{-1}, respectively. Such tandem reaction considering the kinetically labile metal–ligand exchange overcome the drawbacks of direct metal exchange and may be popularized to other systems.

3.4. Modifying surface and interior by tandem PSM

Surface chemistry is crucial for the application of materials. The selective modification of MOF surface and the resulting core–shell structure greatly affect the hydrophobicity, sorption, separation and sensing behaviors. In most reported PSM, the entire framework of the starting MOF was functionalized. Based on the reactivity and spatial effect within the confined channels, rational design of the reaction pathways provides chance to engineer either the surface or interior of MOF.

Wilson and co-workers reported selective surface engineering of a mixed ligands, two-fold interwoven, paddle-wheel MOF [80]. There are trimethylsilyl-protected acetylenes linked to the dipyridine pillars. Tetrabutylammonium fluoride was employed to modify the surface of the reacting crystals by removing the Si group. The large size of the NBu$_4^+$ counterion limits the deprotection just occurring at the external surface, which is confirmed by the evaluation of the Zn/Si ratio before and after reaction. Ethidium bromide monoazide (Eazide) was then attached to terminal alkynes by 'click' reaction. By virtue of the fluorescence of Eazide, confocal microscopy imaging/depth-profiling also verified the surface PSM. After such tandem PSM, the BET surface area of 480 m^2 g^{-1} for the modified compound is comparable to 510 m^2 g^{-1} of the as-synthesized compound, suggesting framework integrity during reaction. The surface terminal alkynes also can react with O-(2-aminoethyl)-O'-(2-azidoethyl)-non-ethylene glycol and changed the MOF surface from hydrophobic to hydrophilic.
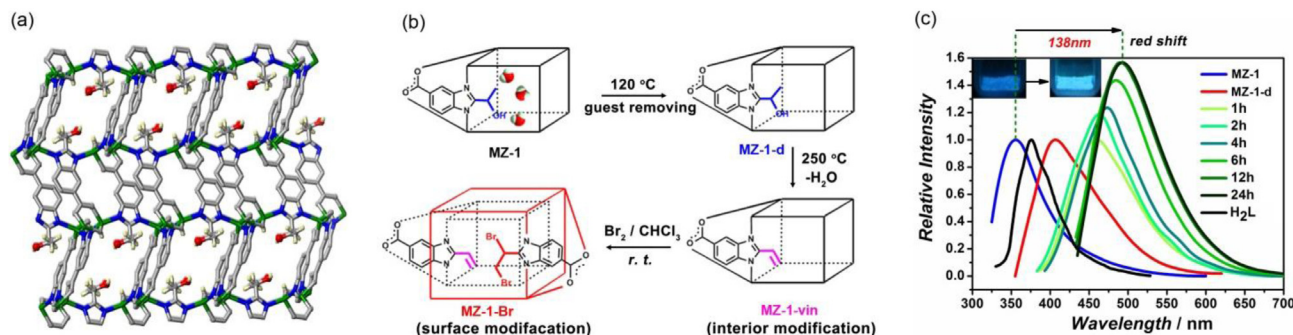
Fig. 12. (a) The structure of **MZ-1** with hydroxyethyl tagged groups hanging in the channels. (b) View of the tandem surface and interior modification by thermal elimination and bromination. (c) Fluorescence change of the MOF during thermal elimination.

Our group reported an example of both surface and interior modification of MOF by tandem reaction of thermal elimination and subsequent bromination (Fig. 12) [32]. A MOF-ZIF structure of MZ-1 with free hydroxyethyl group in channel for further reactions was constructed from a tri-functional imidazole-carboxylate ligand. Hydroxyethyl groups interlaced the two 1D channels along the 110 and -110 directions of the compound. There is a second step in the TGA followed by the guest departure, with an endothermic loss of 3.9% between 250 and 310 °C, which is associated to the dehydration of the $-CHOHCH_3$ to a $-CH{=}CH_2$ group. With preservation of the stable framework, multiple characterizations including ^{13}C NMR, ^1H NMR, liquid chromatography-mass spectrometry confirm the elimination reaction. The solid-to-solid organic reactions were tracked through luminescence change with a major red-shift of 138 nm, due to the increasing conjugation from hydroxyethyl to vinyl. Such luminescence tracking created a very simple but unmasked way to monitor the PSM process of MOF without its destruction. Though it seems quite simple, the vinyl-modified ligand has not been reported. The direct synthesis using both the cyclization reaction and thermal decomposition of the original ligand were infeasible. The synthesis of the vinyl-modified ligand is only possible in a PSM way due to the coordination restriction of the labile carboxylate group. The presence of the unsaturated tag group is suitable to subsequent bromine addition. The framework is preserved with observation of small amount of brominated ligand only at the surface of the crystal due to the steric-hindrance prevented by the newly formed brominated ligand at the channel windows.

The modified MOF shows different absorption behaviors for different guests compared to the parent compound. There is considerable difference in adsorption capacity for gas and solvents, decreasing in an order of MZ-1-d > MZ-1-vin ≫ MZ-1-Br. It is found that gas and solvent molecules exhibit different restoration abilities for the partial distorted channels resulting from thermal induced PSM. Comparing to limited restoration during gas sorption, H_2O and MeOH is capable of full restoration of the channels and bigger EtOH partly restored the channels. In addition, the maximum iodine uptakes of MZ-1-d and MZ-1-vin are comparable, though the iodine sorption rate of MZ-1-d is quicker than that of MZ-1-vin. The surface bromination brings a gate effect, which restrains adsorption for N_2, CO_2 and iodine molecules and suppresses the entrance/releasing of H_2O, MeOH and EtOH. Such stepwise synthetic operations, provides great chance to modify a MOF specific to either the whole framework or regional environment.

3.5. Endowing catalytic activity by tandem PSM

Heterogeneous catalysis is one of the promising applications for MOF due to several advantages such as the high density of active catalytic centers, porosity, enantio-selectivity and re-utilization. Catalytic site stemming from either metals or the organic linkers can be successfully introduced into frameworks via either direct incorporation or PSM, especially by a tandem fashion.

Rosseinsky reported an early example of introducing catalytically active metal complex $VO(acac)_2$ bonded to the linker via two step PSM (Fig. 13a) [81]. IRMOF-3 was first partially converted to modified phase with salicylidene moiety via imine condensation. The resulting IRMOF3-sal$_{0.4}$ was soaked in $VO(acac)_2$, and the vanadium was successfully bonded to the salicylidene moiety. The resulting MOF is an interesting compound processing quite special pore surface with open metal centers, which exhibits catalytic effect for the oxidation of cyclohexene. It is known that the 2-methyl-imidazolate in highly stable ZIF-8 can be exchanged to imidazolate in SALEM-2 with maximum conversation up to 85%. Not only larger pore windows were observed, it also provides additional chance to modify the organic site [61]. Because the linker is activated after coordination, lithiation of the C2 site of im occurred upon exposure to *n*-butyllithium (Fig. 13b). The resulting deproto-
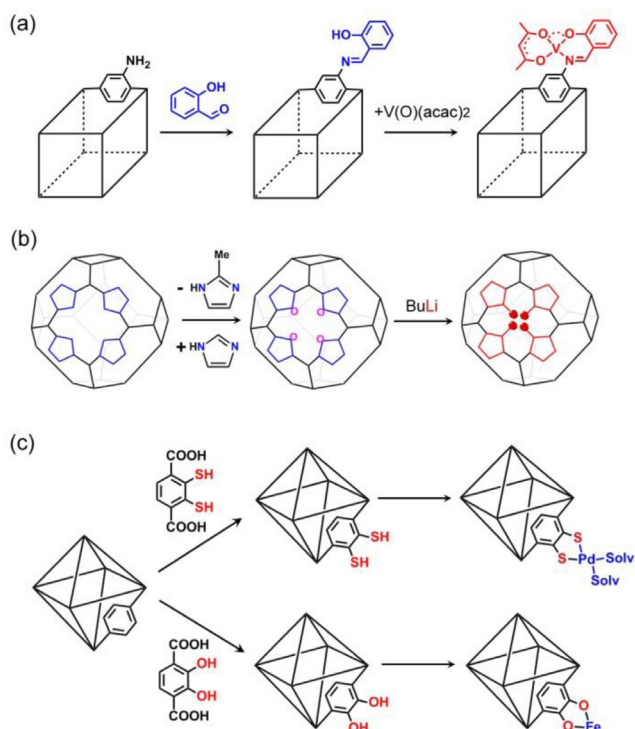

Fig. 13. Introduction of catalytically active site in IRMOF-3 (a), ZIF-8 (b), and UiO-66 (c) by tandem PSM.

nated SALEM-2 is Brønsted-base catalysis for the conjugate addition synthesis of α,β-unsaturated ketone, with percent conversion exceeding 80%. In contrast to SALEM-2, there is no detectable catalytic performance for ZIF-8 under similar conditions.

Recently, Cohen reported the creation of catalytically active metal site by tandem reaction of PSLE followed by metalation (Fig. 13c) [82]. The incorporation of 2,3-dimercapto terephthalate (tcat) into the highly robust UiO-66 was firstly realized via PSLE. The anionic, electron-donating thiocatecholato motif provides an excellent platform to generate site-isolated and unsaturated soft metal sites. Metalation of the -SH group to Pd^{2+} brings rare Pd-mono(tcat) functional group. The Pd-metalated MOF are efficient, heterogeneous, regioselective, and recyclable catalysts. The oxidation of benzo[h]quinoline to install alkoxy groups on a C—H single bond was investigated using the metalated MOF as catalyst, giving nearly quantitative yield of methoxy-functionalized product in 6 h. Although the homogeneous $[Pd(OAc)_2]$ completed the reaction in only ~3 h, UiO-66-PdTCAT exhibited excellent recyclability with holding of high yields exceeding 90%. Similar strategy was also useful for the functionalization of UiO-66 films [83]. Following the substitution of a catechol ligand, $FeCl_3$ metalated the catechol sites and introduced accessible Fe^{3+} centers into the MOF film.

3.6. Multiple magnetic regulations by tandem PSM

Magnetic MOF exhibiting long-range ordering is attractive multifunctional molecular materials [84]. However, tuning the magnetism of a micro-porous magnet is challenging due to the defined metal connection within the framework. Though there are some examples showing modulation of T_C, T_N or magnetic hysteresis, multiple regulation of the ground state is rare. In principle PSM can well modified the magnetic properties from different aspects like spin, change, coordination geometry, and host–guest interaction.

Our group realized a rare and instructive example of magnetism modulation among four magnetic ground states by tandem PSM (Fig. 14) [85]. The rod-space magnetic MOF, $[Co_3^{II}(lac)_2(pybz)_2]\cdot$3DMF (LacCo·3DMF, purple, pybz = 4-pyridyl benzoate, H_2lac = lactic acid) was modified in step-by-step fashion by guest exchange, desolvation, dative PSM and post-synthetic oxidation. A series was generated including $[Co_3^{II}(lac)_2(pybz)_2]\cdot$Guest (Guest = solvents of MeOH, EtOH, PrOH, C_6H_6, and I_2) $[Co_3^{II}(lac)_2(pybz)_2]$ (LacCo, purple), $[Co_3^{II}(pybz)_2(lac)_2(H_2O)_2]\cdot$7$H_2O$ (LacCoa·7H_2O, green) and $[Co^{III}Co_2^{II}(pybz)_2(lac)_2(H_2O)_2]I\cdot$2$H_2O\cdot$1.5DMSO (LacCob·I⁻·2$H_2O\cdot$1.5DMSO, yellow, DMSO = dimethyl sulfoxide). The framework is not altered by the replacement of DMF by different solvents or by the removal of the solvent molecules during the SC–SC transformation. Upon exchange
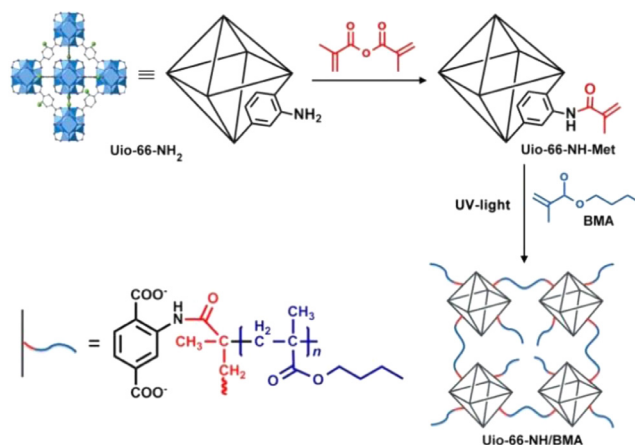

Fig. 15. The strategy to prepare MOF membrane by tandem PSM and the structure view of UiO-66-NH$_2$, UiO-66-NH-Met and UiO-66-NH/BMA membrane. Reproduced from Ref. [86] with Wiley-VCH Verlag GmbH & Co. KGaA, Weinheim.

with H_2O or partial oxidation by molecular iodine, the crystallinity is affected. The magnetic behaviors of the resulting materials are greatly altered by the PSM reactions. LacCo·3DMF and LacCo·Solvent exhibit canted-antiferromagnetism. The long-range magnetic ordering at the temperature of 18 ± 1 K is due to the weak inter-chain (J') interaction stemming from solvents. After desolvation, single-chain magnetic behavior is identified. The H_2O inclusion induces geometry change of the octahedral Co^{2+} and generates a ferrimagnetic ground state. Finally, a ferromagnetic state is stabilized due to the inserting of Co^{3+} at the tetrahedral metal site after iodine oxidation. Such magnetism changing is ascribed to the varying interchain exchanges (J'), antiferromagnetic for LacCo·3DMF and LacCo·Solvent ($J' < 0$), SCM for LacCo (J' verge to 0) and ferromagnetic for LacCoa·7H_2O ($J' > 0$), between adjacent homometal ferrimagnetic chains. For the oxidized compound, there is a turn off of the moment at the tetrahedral site, thus generating a ferromagnetic state ($J' > 0$). Except for the magnetic modulation, the PSM also modified the sorption and electrical behaviors.

3.7. Preparing MOF/polymer hybrid by tandem PSM

As functional materials, an urgent need to push the application of MOF is the transformation of fragile crystalline powders into desired shapes or membranes. Recent advance has confirmed the feasibility of preparing MOF/polymer hybrid by tandem PSM. Wang et al. first reported the preparation of a flexible stand-alone MOF membrane by covalent PSM followed by
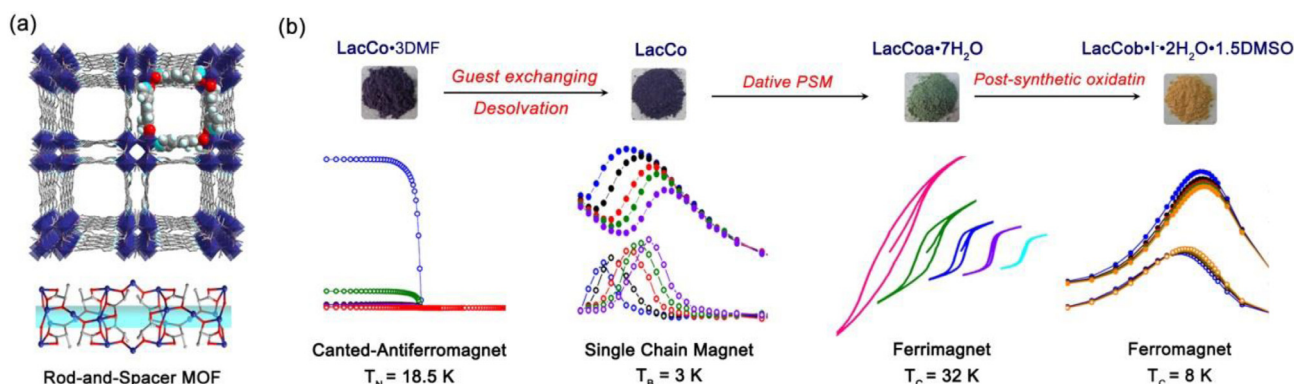

Fig. 14. (a) Structure view of the Rod-and-Spacer MOF with $[Co_3(lac)_2]^{2+}$ chain. (b) Post-synthetic modification induced transformation of four magnetic ground states of canted-antiferromagnet, single chain magnet, ferrimagnet and ferromagnet.

post-synthetic polymerization reaction [86]. Nanosized NH_2-bdc based UiO-66 crystals were synthesized and modified with methacrylic anhydride, resulting in MOF crystals decorated on the ligand struts with terminal, polymerizable olefin groups (Fig. 15). After introduction of butyl methacrylate and photoinitiator, subsequent irradiation with UV light of the suspension results in elastic stand-alone membrane. Such tandem PSM strategy of covalently linking MOF particles through polymer chains prevents troubles like aggregation of small particles and low MOFs/polymers compatibility. Methacrylate derived MOF membrane was also obtained by such tandem PSM. Sorption measurement of the MOFs membrane indicates that the pores of parent MOF are not blocked by the polymer, which is crucial for the application of such MOF/polymer hybrid. The PSM-derived MOF membrane exhibits high separation ability for capturing heavy metal of Cr^{VI} ions from water, giving separation capacity high to 8 mg g^{-1} using the MOF membrane as filter.

In another report, Matzger et al. reported the introduction of a polymer surface of PMMA onto MOF crystal by tandem PSM [87]. A core–shell architecture IRMOF-3@MOF-5 was firstly prepared by growing a shell of IRMOF-3 over a core of MOF-5, which limits the subsequent PSM reaction selectively performing at the external shell. Such a step also overcomes the challenge of decreasing in pore space if solely IRMOF-3 was modified for following polymerization. Reaction of the IRMOF-3 surface with 2-bromoisobutyric anhydride generates ICL@IRMOF-3@MOF-5 bearing a selectively placed polymerization initiator. Copper mediated radical polymerization with methyl methacrylate produces the final product of p oly(methylmethacrylate)@IRMOF-3@MOF-5 with a polymer depth of about 10 μm into the crystal. With a polymer shell, the internal MOF-5 core is unchanged with high accessible porosity. Such hybrid polymer-MOF composite opens new possibility to alter the accessibility of guest molecules to a MOF through the polymer surface.

4. Perspective

Inspiring advance has been achieved in the past five years based on the solid foundation laid by both covalent and dative PSM during the first five years since 2007. The research of PSM has been raised to new heights driven by the collaboration of new post-synthetic methods and tandem reactions. At the most primary level, PSM provides new methods to access crystal engineering beyond synthetic methodology. More importantly, PSM exhibits advantages to address those challenges like introduction of thermo or coordinative active group, creating catalytic site, and improving framework stability. The latest major success of tandem PSM combining different reaction types endow MOF unexpected complexity and show the potential of MOF as idea platform to realize multifunction. It is beyond question that PSM would be absolutely necessary in the future research of MOF.

The history of PSM constantly amends and rebuilds one's view about MOF. Post-synthetic metal and ligand exchanges seem to be a universal phenomenon in MOF. The drastic changes with complex bonds breaking and forming during post-synthetic exchange, confirm the extensive flexibility in crystalline solids. The stable framework connection but liable coordination bonding makes MOF completely new molecular reactant. The spring up of diverse post-synthetic polymerization gradually break the gap between MOF as crystalline solids and soft amorphous polymers, which presents a new and quite practical way to prepare MOF/polymer hybrids.

In the face of great success, challenges remain for the field. For exploring of new reaction types, post-synthetic exchange, elimination, installation and polymerization are just at the very early stage. Present examples mainly focused on some special MOF and rarely cover the mechanism study. There are just limited understanding of the influence of several factors on these new PSM types, which including ionic radii and preferential coordination geometries, size and pKa of the ligand, pore size, framework flexibility and solvent effects. For tandem PSM, it is difficult to in-situ track the PSM process and estimate the time-dependent modification effect, considering MOF is complex heterogeneous system during tandem PSM. There are enormous challenges for current techniques to time-dependently characterize the special domain, surface, local pores of MOF. Precise PSM with high selectivity and controllability is crucial for MOF with desirable function-property combinations. The advance in mechanism study and effect evaluation is urgent desired to pave the way to rational and precise PSM.

Coupling with the appearance of other reaction types and their tandem use in the future, it is suspected that PSM will make progress in several important areas. Post-synthetic exchange/elimination/installation is quite suitable to produce multivariate MOF with different metal ions or ligands in predesigned crystalline lattice. The resulting hybridizing MOF may exhibits synergetic functionality and unusual properties. Post-synthetic elimination/installation tend to play a more significant role in vacancies chemistry, especially in creating and controlling ordered vacancies within MOF. The defects within MOF provide promising chance to tune the electrical, optical, magnetic, and catalytic properties of resulting materials. The great success of systematic installation of various ditopic linker in PCN-700 also suggest an unmissable chance to really control the spatial arrangement of ligand in specially domain, which may bring unprecedented break to MOF. In addition, polymer membrane with high content MOF and MOF@polymer core–shell structure seem to be feasible for wide MOF system, which at least would push the application of MOF on separation and sensing. More broadly, PSM should cover both the physical and chemical changes of the pre-synthesized MOF under external stimulus or with additional reactant. Those wide observed crystalline/solid transformation of MOF, as well as the recent exciting discoveries of MOF glass resulting from melt-quenching of amorphous MOF, can be then viewed as the result of PSM [88]. In a word, the great potential and importance of PSM cannot be overemphasized. We expect more researchers will consider and join in this existing area.

Acknowledgements

References

[1] S. Kitagawa, Acc. Chem. Res. 50 (2017) 514–516.
[2] H. Furukawa, K.E. Cordova, M. O'Keeffe, O.M. Yaghi, Science 341 (2013) 974.
[3] Themed issue of metal-organic frameworks. Chem. Rev. 112 (2012) 673–1268.
[4] Themed issue of metal-organic frameworks. Chem. Soc. Rev. 43 (2014) 5415–6172.
[5] Themed issue of metal-organic frameworks. Chem. Soc. Rev. 38 (2009) 1201–1508.
[6] M. O'Keeffe, M.A. Peskov, S.J. Ramsden, O.M. Yaghi, Acc. Chem. Res. 41 (2008) 1782–1789.
[7] H.L. Jiang, T.A. Makala, H.C. Zhou, Coord. Chem. Rev. 257 (2013) 2232–2249.
[8] S. Horike, S. Shimomura, S. Kitagawa, Nat. Chem. 1 (2009) 695–704.
[9] N. Ko, Y.B. Go, N. Aratani, S.B. Choi, E.A. Choi, O.M. Yaghi, Science 329 (2010) 424–428.
[10] T.D. Bennett, J.C. Tan, Y. Yue, E. Baxter, C. Ducati, N.J. Terrill, H.H. Yeung, Z. Zhou, W. Chen, S. Henke, A.K. Cheetham, G.N. Greaves, Nat. Commun. 6 (2015) 8079.

[11] L. Ma, J.M. Falkowski, C. Abney, W. Lin, Nat. Chem. 2 (2010) 838–846.
[12] S. Yang, X. Lin, A.J. Blake, G.S. Walker, P. Hubberstey, N.R. Champness, M. Schroeder, Nat. Chem. 1 (2009) 487–493.
[13] P. Ramaswamy, N.E. Wong, B.S. Gelfand, G.K.H. Shimizu, J. Am. Chem. Soc. 137 (2015) 7640–7643.
[14] H.J. Son, S.Y. Jin, S. Patwardhan, S.J. Wezenberg, N.C. Jeong, M. So, C.E. Wilmer, A.A. Sarjeant, G.C. Schatz, R.Q. Snurr, O.K. Farha, G.P. Wiederrecht, J.T. Hupp, J. Am. Chem. Soc. 135 (2013) 862–869.
[15] P.Q. Liao, N.Y. Huang, W.X. Zhang, J.P. Zhang, X.M. Chen, Science 356 (2017) 1193–1196.
[16] D.W. Fu, H.L. Cai, Y. Liu, Q. Ye, W. Zhang, Y. Zhang, X.Y. Chen, G. Giovannetti, M. Capone, J. Li, R.G. Xiong, Science 339 (2013) 425.
[17] Y. Liu, W.M. Xuan, Y. Cui, Adv. Mater. 22 (2010) 4112–4135.
[18] H.L. Guo, Y.Z. Zhu, S.L. Qiu, J.A. Lercher, H.J. Zhang, Adv. Mater. 37 (2010) 4190.
[19] Z. Wang, S.M. Cohen, Chem. Soc. Rev. 38 (2009) 1315–1329.
[20] S.M. Cohen, Chem. Rev. 112 (2012) 970–1000.
[21] M. Lalonde, W. Bury, O. Karagiaridi, Z. Brown, J.T. Hupp, O.K. Farha, J. Mater. Chem. A 1 (2013) 5453.
[22] C.K. Brozek, M. Dinca, Chem. Soc. Rev. 43 (2014) 5456–5467.
[23] J.D. Evans, C.J. Sumby, C.J. Doonan, Chem. Soc. Rev. 43 (2014) 5933–5951.
[24] P. Deria, J.E. Mondloch, O. Karagiaridi, W. Bury, J.T. Hupp, O.K. Farha, Chem. Soc. Rev. 43 (2014) 5896–5912.
[25] O. Karagiaridi, W. Bury, J.E. Mondloch, J.T. Hupp, O.K. Farha, Angew. Chem. 53 (2014) 4530–4540.
[26] S.M. Cohen, J. Am. Chem. Soc. 139 (2017) 2855–2863.
[27] B.F. Hoskins, R. Robson, J. Am. Chem. Soc. 112 (1990) 1546.
[28] Y.H. Kiang, G.B. Gardner, S. Lee, Z. Xu, E.B. Lobkovsky, J. Am. Chem. Soc. 121 (1999) 8204.
[29] J.S. Seo, D. Whang, H. Lee, S.I. Jun, J. Oh, Y.J. Jeon, K. Kim, Nature 404 (2000) 982.
[30] Z.Q. Wang, S.M. Cohen, J. Am. Chem. Soc. 129 (2007) 12368–12369.
[31] M. Zhang, T. Yang, Z. Wang, X.F. Ma, Y. Zhang, S.M. Greer, S.A. Stoian, Z.W. Ouyang, H. Nojiri, M. Kurmoo, M.H. Zeng, Chem. Sci. 8 (2017) 5356–5361.
[32] F. Sun, Z. Yin, Q.Q. Wang, D. Sun, M.H. Zeng, M. Kurmoo, Angew. Chem. Int. Ed. 52 (2013) 4538–4543.
[33] D. Liu, Z.G. Ren, H.X. Li, J.P. Lang, N.Y. Li, B.F. Abrahams, Angew. Chem. Int. Ed. 49 (2010) 4767–4770.
[34] Z. Yin, M.H. Zeng, Sci. China Chem. (2011) 1371–1394.
[35] L. Mi, H. Hou, Z. Song, H. Han, H. Xu, Y. Fan, S.W. Ng, Cryst. Growth Des. 7 (2007) 2553–2561.
[36] X. Song, S. Jeong, D. Kim, M.S. Lah, CrystEngComm 14 (2012) 5753–5756.
[37] T.K. Prasad, D.H. Hong, M.P. Suh, Chem. Eur. J. 16 (2010) 14043–14050.
[38] Q.X. Yao, J.L. Sun, K. Li, J. Su, M.V. Peskova, X.D. Zou, Dalton Trans. 41 (2012) 3953–3955.
[39] X. Song, T.K. Kim, H. Kim, D. Kim, S. Jeong, H.R. Moon, M.S. Lah, Chem. Mater. 24 (2012) 3065–3073.
[40] Z.W. Wei, W.G. Lu, H.L. Jiang, H.C. Zhou, Inorg. Chem. 52 (2013) 1164–1166.
[41] Z.J. Zhang, W. Shi, Z. Niu, H.H. Li, B. Zhao, P. Cheng, D.Z. Liao, S.P. Yan, Chem. Commun. 47 (2011) 6425–6427.
[42] T.F. Liu, L. Zou, D. Feng, Y.P. Chen, S. Fordham, X. Wang, Y. Liu, H.C. Zhou, J. Am. Chem. Soc. 136 (2014) 7813–7816.
[43] P.Á. Szilágyi, P. Serra-Crespo, I. Dugulan, J. Gascon, H. Geerlings, B. Dam, CrystEngComm 15 (2013) 10175–10178.
[44] C.K. Brozek, M. Dinca, Chem. Sci. 3 (2012) 2110–2113.
[45] C.K. Brozek, M. Dinca, J. Am. Chem. Soc. 135 (2013) 12886–12891.
[46] S. Das, H. Kim, K. Kim, J. Am. Chem. Soc. 131 (2009) 3814–3815.
[47] M. Dinca, J.R. Long, J. Am. Chem. Soc. 129 (2007) 11172–11176.
[48] K. Sumida, D. Stuck, L. Mino, J.D. Chai, E.D. Bloch, O. Zavorotynska, L.J. Murray, M. Dinca, S. Chavan, S. Bordiga, M. Head-Gordon, J.R. Long, J. Am. Chem. Soc. 135 (2013) 1083–1091.
[49] D. Denysenko, T. Werner, M. Grzywa, A. Puls, V. Hagen, G. Eickerling, J. Jelic, K. Reuter, D. Volkmer, Chem. Commun. 48 (2012) 1236–1238.
[50] C.J. Hafizovic, S. Jakobsen, U. Olsbye, N. Guillou, C. Lamberti, S. Bordiga, K.P. Lillerud, J. Am. Chem. Soc. 130 (2008) 13850–13851.
[51] M. Kim, J.F. Cahill, H. Fei, K.A. Prather, S.M. Cohen, J. Am. Chem. Soc. 134 (2012) 18082–18088.
[52] J. Kahr, R.E. Morris, P.A. Wright, CrystEngComm 15 (2013) 9779–9786.
[53] Z. Zhang, L. Zhang, L. Wojtas, P. Nugent, M. Eddaoudi, M.J. Zaworotko, J. Am. Chem. Soc. 134 (2012) 924–927.
[54] Z. Zhang, L. Wojtas, M. Eddaoudi, M.J. Zaworotko, J. Am. Chem. Soc. 135 (2013) 5982–5985.
[55] R. Kitaura, F. Iwahori, R. Matsuda, S. Kitagawa, Y. Kubota, M. Takata, T.C. Kobayashi, Inorg. Chem. 43 (2004) 6522–6524.
[56] J.R. Li, H.C. Zhou, Nat. Chem. 2 (2010) 893–898.
[57] B.J. Burnett, P.M. Barron, C. Hu, W. Choe, J. Am. Chem. Soc. 133 (2011) 9984–9987.
[58] W. Bury, D. Fairen-Jimenez, M.B. Lalonde, R.Q. Snurr, O.K. Farha, J.T. Hupp, Chem. Mater. 25 (2013) 739–744.
[59] C.Y. Lee, O.K. Farha, B.J. Hong, A.A. Sarjeant, S.T. Nguyen, J.T. Hupp, J. Am. Chem. Soc. 133 (2011) 15858–15861.
[60] O. Karagiaridi, W. Bury, A.A. Sarjeant, C.L. Stern, O.K. Farha, J.T. Hupp, Chem. Sci. 3 (2012) 3256–3260.
[61] O. Karagiaridi, M.B. Lalonde, W. Bury, A.A. Sarjeant, O.K. Farha, J.T. Hupp, J. Am. Chem. Soc. 134 (2012) 18790–18796.
[62] B.B. Tu, Q.Q. Pang, D.F. Wu, Y. Song, L.H. Weng, Q.W. Li, J. Am. Chem. Soc. 136 (2014) 14465–14471.
[63] S. Surble, C. Serre, C. Mellot-Draznieks, F. Millange, G. Ferey, Chem. Commun. (2006) 284–286.
[64] Y.S. Wei, M. Zhang, P.Q. Liao, R.B. Lin, T.Y. Li, G. Shao, J.P. Zhang, X.M. Chen, Nat. Commun. 6 (2015) 8348.
[65] S. Yuan, W.G. Lu, Y.P. Chen, Q. Zhang, T.F. Liu, D.W. Feng, X. Wang, J.S. Qin, H.C. Zhou, J. Am. Chem. Soc. 137 (2015) 3177–3180.
[66] S. Yuan, Y.P. Chen, J.S. Qin, W.G. Lu, L.F. Zou, Q. Zhang, X. Wang, X. Sun, H.C. Zhou, J. Am. Chem. Soc. 138 (2016) 8912–8919.
[67] C.X. Chen, Z. Wei, J.J. Jiang, Y.Z. Fan, S.P. Zheng, C.C. Cao, Y.H. Li, D. Fenske, C.Y. Su, Angew. Chem. Int. Ed. 55 (2016) 9932–9936.
[68] Z.Q. Wang, S.M. Cohen, Angew. Chem. Int. Ed. 47 (2008) 4699–4702.
[69] M. Savonnet, D.B. Bachi, N. Bats, J. Perez-Pellitero, E. Jeanneau, V. Lecocq, C. Pinel, D. Farrusseng, J. Am. Chem. Soc. 132 (2010) 4518–4519.
[70] A. Kronast, S. Eckstein, P.T. Altenbuchner, K. Hindelang, S.I. Vagin, B. Rieger, Chem. Eur. J. 22 (2016) 12800–12807.
[71] H. Liu, F.G. Xi, W. Sun, N.N. Yang, E.Q. Gao, Inorg. Chem. 55 (2016) 5753–5755.
[72] A.S. Bernt, V. Guillerm, C. Serre, N. Stock, Chem. Commun. 47 (2011) 2838–2840.
[73] S.J. Garibay, Z. Wang, K.K. Tanabe, S.M. Cohen, Inorg. Chem. 48 (2009) 7341–7349.
[74] A.M. Fracaroli, P. Siman, D.A. Nagib, M. Suzuki, H. Furukawa, F.D. Toste, O.M. Yaghi, J. Am. Chem. Soc. 138 (2016) 8352–8355.
[75] T. Li, M.T. Kozlowski, E.A. Doud, M.N. Blakely, N.L. Rosi, J. Am. Chem. Soc. 135 (2013) 11688–11691.
[76] C. Liu, T.Y. Luo, E.S. Feura, C. Zhang, N.L. Rosi, J. Am. Chem. Soc. 137 (2015) 10508–10511.
[77] C. Liu, C. Zeng, T.Y. Luo, A.D. Merg, R. Jin, N.L. Rosi, J. Am. Chem. Soc. 138 (2016) 12045–12048.
[78] Z. Yin, Y.L. Zhou, M.H. Zeng, M. Kurmoo, Dalton Trans. 44 (2015) 5258–5275.
[79] J.H. Cavka, S. Jakobsen, U. Olsbye, N. Guillou, C. Lamberti, S. Bordiga, K.P. Lillerud, J. Am. Chem. Soc. 130 (2008) 13850–13851.
[80] T. Gadzikwa, G. Lu, C.L. Stern, S.R. Wilson, J.T. Hupp, S.T. Nguyen, Chem. Commun. (2008) 5493–5495.
[81] M.J. Ingleson, J.P. Barrio, J.B. Guilbaud, Y.Z. Khimyak, M.J. Rosseinsky, Chem. Commun. (2008) 2680–2682.
[82] H. Fei, S.M. Cohen, J. Am. Chem. Soc. 137 (2015) 2191–2194.
[83] H. Fei, S. Pullen, A. Wagner, S. Ott, S.M. Cohen, Chem. Commun. 51 (2015) 66–69.
[84] P. Dechambenoit, J.R. Long, Chem. Soc. Rev. 40 (2011) 3249–3265.
[85] M.H. Zeng, Z. Yin, Y.X. Tan, W.X. Zhang, Y.P. He, M. Kurmoo, J. Am. Chem. Soc. 136 (2014) 4680–4688.
[86] Y.Y. Zhang, X. Feng, H.W. Li, Y.F. Chen, J.S. Zhao, S. Wang, L. Wang, B. Wang, Angew. Chem. Int. Ed. 54 (2015) 4259–4263.
[87] K.A. McDonald, J.I. Feldblyum, K. Koh, A.G. Wong-Foy, A.J. Matzger, Chem. Commun. 51 (2015) (1996) 11994–11996.
[88] T.D. Bennett, A.K. Cheetham, Acc. Chem. Res. 47 (2014) 1555–1562.